Post-print version: Jimenez-Vicaria, J. D., Castro-Fresno, D., & G. Pulido, M. D. (2020). Fatigue behaviour of adhesive bonds in tensile CFRP-metal double-strap joints with puddle iron plates taken from a 19th century bridge. Composite Structures, 251 doi:10.1016/j.compstruct.2020.112600

Fatigue behaviour of adhesive bonds in tensile CFRP-metal double-strap joints with puddle iron plates taken from a 19th century bridge

Jimenez-Vicaria, J. David[1, 2*]; Castro-Fresno, Daniel[3]; G. Pulido, M. Dolores[4]

1: Centro Tecnológico. ACCIONA Construcción. Valportillo Segunda 8, 28108 Alcobendas (Spain)
e-mail: josedavid.jimenez.vicaria@acciona.com

2: GITECO. Universidad de Cantabria. Avda. de los Castros 44, 39005 Santander (Spain)
e-mail: jose-david.jimenez@alumnos.unican.es

3: GITECO. Universidad de Cantabria. Avda. de los Castros 44, 39005 Santander (Spain)
e-mail: castrod@unican.es

4: Instituto CC Eduardo Torroja – CSIC. Serrano Galvache 4, 28033 Madrid (Spain)
e-mail: dpulido@ietcc.csic.es

Abstract

The use of adhesively-bonded CFRP crack-patching in old metallic bridges seems to be a promising fatigue strengthening technique, but the internal laminar structure of puddle iron could influence its efficiency, resulting in premature interlaminar failure within the metal before CFRP debonding. To investigate the fatigue behaviour of this retrofitting system, six double-strap joints with CFRP laminates adhesively-bonded to puddle iron plates taken from a 19th century bridge were tested. Three specimens were statically loaded until failure as control specimens, and other three were tested under tensile-tensile fatigue loading up to 2 million cycles at a frequency of 10 Hz, with stress ranges in the metal of 60, 75 and 90 MPa. An analytical model is used to compute the maximum principal stress range in the adhesive during fatigue loading, which is assumed as the governing fatigue strength parameter in the double-strap joint. Based on the experimental results of the present work, together with a database for joints with modern steel collected from literature, an S-N fatigue curve is obtained for CFRP-metal double-strap specimens, and a fatigue limit in terms of maximum principal stress range in the adhesive layer is proposed to be used in design guidelines.

Keywords: CFRP-metal adhesive joints; Fatigue test; S–N curve; puddle iron; strengthening

1. Introduction

Many old metallic bridges constructed during the second half of the 19th century up to the middle of the 20th century are still in operation and are now reaching the end of their expected fatigue life. Since these bridges have been subjected to increasing traffic loads along their service lives, they require maintenance and rehabilitation works in order to postpone their replacement by new bridges [1].

The traditional repairing method for extending the fatigue life of metallic bridges is based on the use of steel plates attached to the damaged structural element by welding or bolting [2]. However, metals from the end of 19th century to the beginning of 20th century used for bridge construction are not suitable for welding due to a differentiated toughness, which means that cracks can originate due to the residual stresses from the heat-affected zone of the weld [3]. Moreover, this strengthening method is usually quite expensive and time-consuming, and shows several disadvantages [4] such as the introduction of additional permanent loads and new stress concentration areas, and also the additional steel plates are subjected to the same phenomena of fatigue and corrosion. These negative effects can be avoided using CFRP laminates, as this is an effective strengthening system with high tensile strength and stiffness, that can be readily implemented on field, minimizes the dead weight increment, reduces the traffic disruption and offers good durability properties [5], [6], [7].

Most previous studies on the topic have mainly focused on the static behaviour of CFRP strengthened steel structures [8], [9], and some others have evaluated the fatigue behaviour of CFRP laminates bonded to steel substrates [10], [11]. However, only few have focused on the fatigue behaviour of old metallic structures strengthened with CFRP [12], [13]. Generally, CFRP laminates have a good fatigue resistance for in-plane loads parallel to the fibre direction [14], so the CFRP is not generally a fatigue critical issue in this structural strengthening system. However, the efficiency of fatigue strengthening depends on the bond performance between the CFRP and the metal, so the fatigue loading effects on the bonding need to be considered.

During the second half of the 19th century, puddle iron was the material used for the construction of metallic bridges until it was replaced by old steel at the beginning of the 20th century. The manufacturing process of this metal led to the formation of high concentrations of unwanted compounds, resulting in a banded structure with large slag inclusions [3]. This internal laminar structure in the puddle iron could be a potential problem when considering CFRP strengthening, since delamination under interlaminar shear within the puddle iron plate would be a similar phenomenon to debonding of CFRP at the CFRP-metal interface, especially under fatigue loads [15].

These particular properties of puddle iron could influence the effect of fatigue loading on the bond behaviour between CFRP and the metal in old metallic bridges strengthened with this material.

This lack of knowledge motivates the present work, in which an experimental campaign is carried out to investigate the fatigue behaviour of the adhesive bonds in tensile CFRP-metal double-strap joints with puddle iron plates taken from a bridge built in the 19th century. These specimens can be considered representative of CFRP crack-patching sections under tension in old metallic bridges that need to be repaired. The experimental results are then compared with those for joints with modern steel reported in literature, evaluating the S-N fatigue curves and defining a fatigue limit for CFRP-metal double-strap specimens that could be used in design guidelines.

2. Experimental program

2.1. Specimen preparation

In the present study, six double-strap joints with CFRP laminates adhesively-bonded to puddle iron plates taken from a 19th century bridge were prepared. Three of them were tested under static loading until failure as control specimens (S1, S2 and S3) and other three under tensile-tensile fatigue loading (F1, F2 and F3) up to 2 million cycles at a frequency of 10 Hz. The number of cycles was selected based on the definition of *reference fatigue strength* for a particular detail in Eurocode 3: the constant amplitude stress range $\Delta\sigma_s$ in the metal for an endurance N = $2x10^6$ cycles [16]. Those specimens which survived the fatigue cycles were later tested under static loading until failure to compare the results with control specimens so that the effect of fatigue loading on the bond behaviour could be examined. All six specimens had the same geometry, as shown in Fig. 1, with a bond length of 60 mm. In order to ensure that the failure occurred on the desired side of the specimen (the 60 mm side in Fig. 1), a longer bond length of 90 mm was applied at the other side of the joint gap. In addition, a bond length of 60 mm was selected so that the results from this study can be compared with the results of a previous research by the authors reported in [17] for double-strap joints with modern steel using the same combination of CFRP and adhesive.

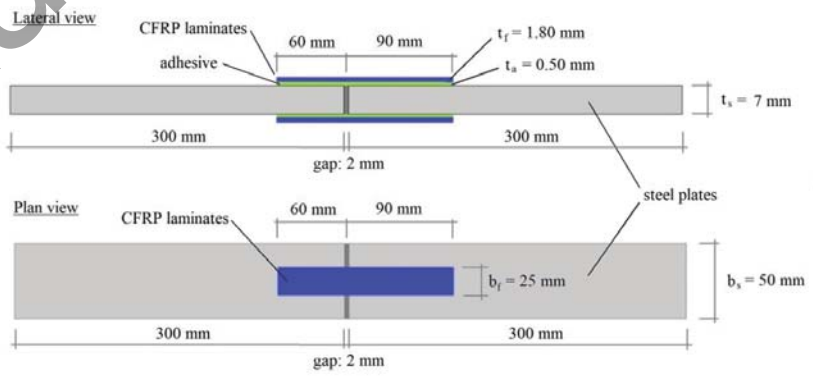

Fig. 1

The puddle iron plates used to fabricate the double-strap specimens were cut by water-jetting from the web of four stringers that were extracted during rehabilitation works in 2017 from an old riveted metallic railway bridge (Fig. 2) that was built in Redondela (Pontevedra, Spain) in 1884.

Fig. 2

To prepare the double-strap joint specimens, first the surface of metallic plates was grit blasted with aluminium silica (Fig. 3a), since it has been demonstrated to be the most effective surface treatment for the metal [18]. The surfaces were then cleaned with acetone immediately before the adhesive application. After that, two metallic plates are aligned, maintaining a gap of 2 mm between them by means of a neoprene joint. Immediately after the metallic surface preparation (within the first 12 hours) an adhesive layer was applied uniformly on both the surface of the metal and the CFRP laminate, in order to avoid any possible contamination. Next, the CFRP laminate was positioned on the surface of the metallic plate (Fig. 3b), and uniform pressure was applied to remove the excess of adhesive, until the desired adhesive thickness was achieved. To control the correct alignment of the specimen and the thickness of the adhesive, an alignment tool and a series of separators were used to maintain a 0.5 mm theoretical fixed thickness of adhesive during the preparation (Fig. 3b).

The specimens were cured in an oven at 50ºC during 16 hours. Differential Scanning Calorimetry tests using DSC Q-200 were performed on adhesive samples cured in the oven under the same conditions of double-strap joints to obtain the glass transition temperature (T_g) of the adhesive used to bond the CFRP laminates to the metal. An average value of 58ºC was obtained, with a coefficient of variation of 9.5%. This temperature should not be attained during fatigue testing since it could affect the bond behaviour, so thermocouples were used during fatigue tests to monitor the temperature in the joint during fatigue cycles.

a) Grit blasting of metallic surface

b) Bonding of CFRP laminates on metal

Fig. 3

136

137 *2.2. Material properties*

138

139 The puddle iron plates had a length, width and thickness of 300 mm, 50 mm and 7 mm,
140 respectively (Fig. 1). The width of these metallic plates was selected so that the metal did not
141 yield during the double-strap joint tests. From tensile tests on five puddle iron coupons (tested
142 according to UNE-EN 6892-1 [19]), an average tensile modulus of elasticity, yield stress, tensile
143 strength and elongation at break of 198 GPa, 313 MPa, 367 MPa and 9.04% was obtained (Table
144 1). According to Charpy impact tests (UNE-EN ISO 148 [20]), an average impact energy of 6.3
145 J resulted from nine specimens, with a coefficient of variation of 45 % (this significant coefficient
146 of variation in the impact energy can be attributed to the high heterogeneities in the material
147 microstructure). A significant amount of longitudinal non-metallic inclusions can be observed in
148 Fig. 4, typically composed of phosphorus and sulphur (it was found that the phosphorus content
149 in this metal is significant in comparison with modern steels, Table 1). These inclusions are
150 considered to be responsible for the embrittlement of this low-carbon content metal [21], which
151 is supported by the lower elongation at break and lower toughness obtained for this metal
152 compared to modern steel (Table 1).
153 CFRP laminates of 1.80 mm nominal thickness, 25 mm width and 150 mm length were used (Fig.
154 1), manufactured by resin infusion with a two-part epoxy resin (Araldite® LY 1568/Aradur® 3489)
155 on unidirectional carbon fibre fabrics with Pyrofil™ HR40 fibres, and cured at 80ºC during 4
156 hours, according to manufacturer recommendations. From tensile tests on standardized specimens
157 according to ASTM-D3039 [22], the modulus of elasticity, tensile strength, strain at failure and
158 Poisson coefficient of CFRP laminates were experimentally determined, obtaining values of
159 183.61 GPa, 1663 MPa, 0.91% and 0.328, respectively (Table 1).
160 As structural epoxy adhesive for bonding the CFRP laminates to the metallic plates, Araldite®
161 2031 was used, and its mechanical properties were obtained experimentally from tensile tests
162 according to ASTM-D638 standard [23], with an average modulus of elasticity, tensile strength
163 and ultimate tensile strain of 1451 MPa, 19 MPa and 2.98%, respectively.

The selection of this CFRP laminate and epoxy adhesive was based on the results of an experimental campaign carried out by the authors to study the influence of carbon fibre stiffness and adhesive ductility on CFRP-metal adhesive joints [17]. The measured material properties of puddle iron plates, CFRP laminates and adhesive are listed in Table 1. Tensile stress-strain curves for the puddle iron, CFRP and adhesive are reported in Fig. 5.

Table 1. Material properties of puddle iron and modern steel plates, CFRP laminate and adhesive.

	Puddle iron	Modern Steel [4]	CFRP	Adhesive
Tensile strength (MPa)	367 [1]	410-560	1663	19
Yield strength (MPa)	313 [1]	>275	N/A	N/A
Tensile modulus (GPa)	198 [1]	210	183.6	1.45
Elongation at break (%)	9.04 [1]	>23	0.91	2.98
Poisson's ratio	0.3 [3]	0.3	0.328	0.35[1]
Toughness (J) [2]	6.3	>27	-	-

[1] Average values based on 5 specimens, tested according to UNE-EN 6892-1 [19]

[2] According to UNE-EN ISO 148 [20] (test temperature 0°C)

[3] Assumed value (not measured during tests)

[4] According to UNE-EN 10025-2 [24]

Table 2. Chemical composition (in % weight) of tested puddle iron and typical modern steel.

	C	Si	Mn	P	S
Investigated puddle iron *	0.02	0.17	0.04	>0.12	0.04
Typical values for modern steel **	<0.21	Variable	<1.50	<0.04	<0.04

** Average values from two specimens taken from Redondela stringers*

*** Hot rolled, non-alloy structural steel S 275 JR (according to EN 10025-2 [24])*

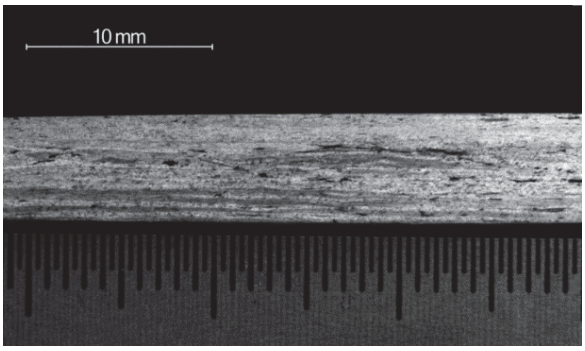

a) Banded structure with large slag inclusions

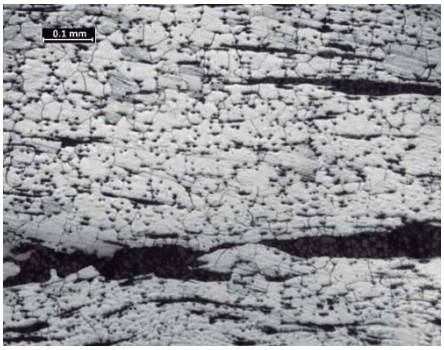

b) x100 image

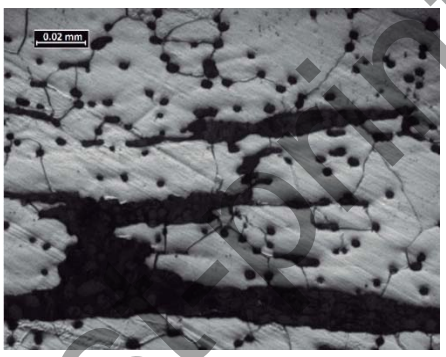

c) x500 image

Fig. 4

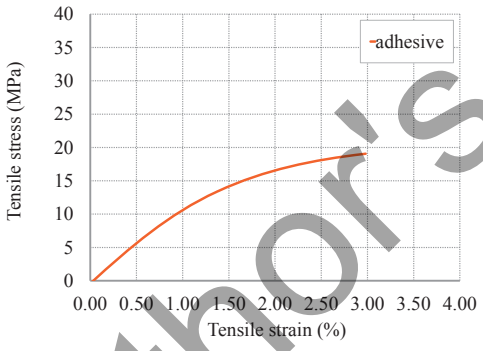

a) Adhesive

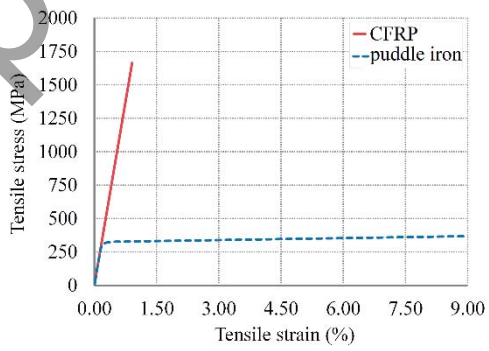

b) CFRP and puddle iron

Fig. 5

3. Experimental results

3.1. Static tests

Three control specimens were tested under static loading until failure to obtain the static bond strength $P_{u,static}$ and to analyse the failure mode of double-strap joints in case of puddle iron, so it can be compared to the behaviour of specimens with modern steel. All tests were carried out in tensile using an Instron 3382 multitest press, in displacement control at a loading rate of 0.5 mm/min until failure. The average failure load was 69.24 kN, with a deviation of 2.7 %. Based

on this result, it can be noticed that a double-strap joint with puddle iron has an average static bond strength consistent with results reported in previous research [17] with modern steel specimens with the same geometry and same CFRP and adhesive. In specimens with modern steel [17], an average static bond strength of 61.85 kN was obtained (10.7 % lower, a difference that can be attributed to the inherent variability of the strength of these joints). The instrumentation and test set-up for the specimens tested under static loading are shown in Fig. 6.

a) Specimen S1 b) Specimen S2 c) Detail of strain gauges

Fig. 6

These specimens were instrumented by strain gauges attached to the CFRP at the joint location (gauges *G2* and *G4*, one gauge at each face of the specimen) to measure the stains in both CFRP laminates during loading (Fig. 6). Similarly, other two strain gauges were placed on the metal at 20 mm from the CFRP laminate end (gauges *G1* and *G3*) to measure the strain in the metallic plate. The strain measures can be used to check the eccentricity of the applied tensile force and the load transferred from the metal to the CFRP by means of the adhesive bond. As can be seen in Table 3 and Fig. 7b, in specimen S2 it is clear that there was bending during testing, as the difference in strain between the two faces of the specimen was considerable (29.5% in the metal strain and 36.6% in the CFRP strain, at failure load), so this result was discarded and not considered to obtain the average static bond strength. This bending during testing, that can be attributed to a misalignment during specimen preparation, justifies the lower failure load in this specimen S2 (23.3 % reduction), compared to the other two results. The load-strain curves from tensile static tests are shown in Fig. 7 for both the metal strains ε_{metal} and CFRP strains ε_{CFRP} in specimens S1 and S3, computed as the average of strains measured at both specimen faces (Fig. 7a), while for specimen S2 it is shown at each face (A and B) separately to reflect the bending during loading (Fig. 7b). Face A of the specimen is the frontal one (visible in Fig. 6), while face B is the back one (not visible).

Table 3. Test results of static tests control specimens.

Specimen	t_a	$P_{u,static}$	$G1$	$G3$	E_{metal}	$\Delta\varepsilon_{metal}$	$G2$	$G4$	ε_{CFRP}	$\Delta\varepsilon_{CFRP}$
	mm	kN	με	με	με	%	με	με	με	%
S-1	0.48	70.55	1189	1168	1179	-1.8	3715	3643	3679	-1.9
S-2	0.54	53.08	743	962	853	29.5	3392	2152	2772	-36.6
S-3	0.54	67.92	1054	1137	1096	7.9	3366	3449	3408	2.5

Where t_a is the measured adhesive thickness; ε_{metal} and ε_{CFRP} are the average metal and CFRP strains measured at both specimen faces, respectively; and $\Delta\varepsilon_{metal}$ and $\Delta\varepsilon_{CFRP}$ are the difference in metal and CFRP strains between the two faces of the specimen, respectively.

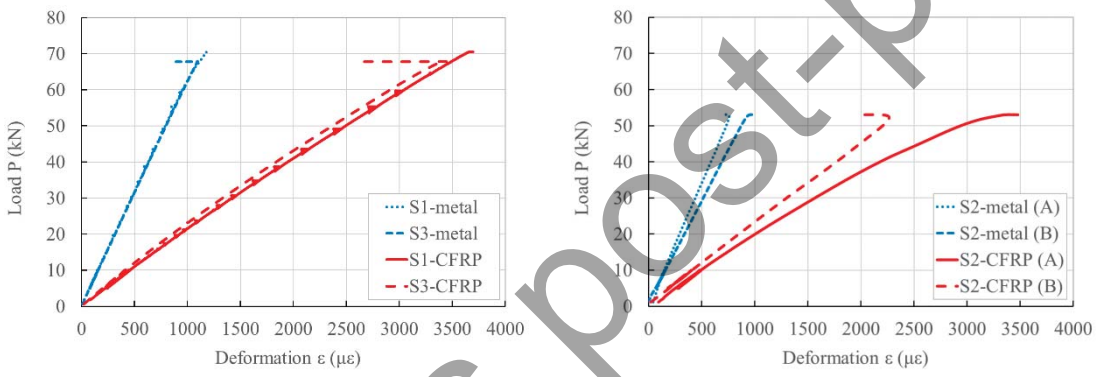

a) Specimens S1 and S3 b) Specimen S2

Fig. 7

3.2. Fatigue tests

Specimens F1, F2 and F3 were subjected to 2 million fatigue loading cycles in an Instron® 8802 Servohydraulic Fatigue Testing System with a loading capacity of 250 kN (Fig. 8). The loading frequency was selected equal to 10 Hz, as it is within the ranges in which temperature increases is not expected to adversely affect the strength of the joint. The stress ratio, defined as the ratio between the minimum and maximum load during fatigue test (P_{min}/P_{max}), was set in all cases as $R = 0.1$, as it is frequently used in literature. The specimens F1, F2 and F3 were subjected to a constant sinusoidal tensile stress range in the metal $\Delta\sigma_s$ of 60, 75 and 90 MPa, respectively, which corresponds to a load ratio $P_{max}/P_{u,static}$ of 0.33, 0.42 and 0.51, respectively. These values were adopted since fatigue is developed under service loads, which are usually below 50% of ultimate loads. In fact, [5] recommend that the maximum load during fatigue test P_{max} should not exceed 30-40% of the static bond strength $P_{u,static}$, but in this case it was decided to test a specimen under higher loads (F3).

Those specimens which survived the 2 million cycles fatigue loading (F1 and F2) were tested until failure under static loading at an extension rate of 0.5 mm/min using the same testing machine. The load-extension curves of these tests is shown in Fig. 9, being P the load applied by the testing machine and δ the extension of the specimen (measured as the separation between the grippers of the testing machine). By comparing the static failure load before and after fatigue tests, the effect of fatigue loading on the bond behaviour between CFRP laminates and puddle iron plates can be investigated.

a) Specimen F1 b) Specimen F2 c) Specimen F3

Fig. 8

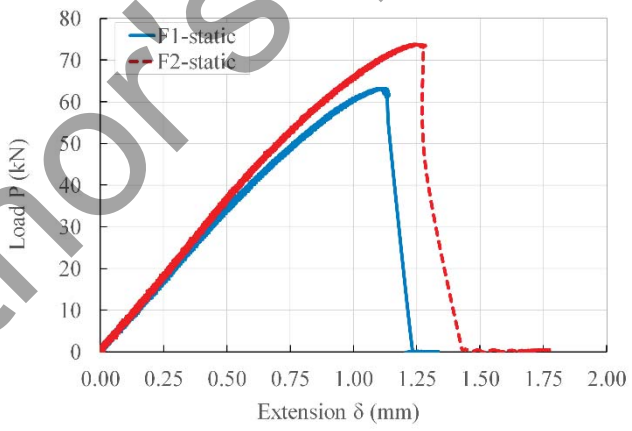

Fig. 9

For each specimen, the applied load cycles (up to 2 million), the fatigue stress range in the bare metal section and the residual static bond strength after 2 million fatigue cycles $P_{u,fatigue}$ are reported in Table 4.

Table 4. Test results of fatigue specimens.

Spec.	t_a	P_{min}	P_{max}	ΔP	$\Delta\sigma_s$	P_{min}/P_{max}	$P_{max}/P_{u,static}$	N_{cycles}	$P_{u,fatigue}$	$P_{u,fatigue}/P_{u,static}$
	mm	kN	kN	kN	MPa				kN	
F-1	0.71	2.3	23.0	20.7	60	0.1	0.33	2,000,000	63.1	0.91
F-2	0.87	2.9	29.0	26.1	75	0.1	0.42	2,000,000	73.7	1.06
F-3	0.53	3.5	35.0	31.5	90	0.1	0.51	323,384	-	-

Where t_a is the adhesive layer thickness; P_{min} is the minimum load during fatigue test; P_{max} is the maximum load during fatigue test; $\Delta P = P_{max} - P_{min}$ is the fatigue load range; $\Delta\sigma_s$ is the fatigue stress range in metal; $R = P_{min}/P_{max}$ is the stress ratio; $P_{max}/P_{u,static}$ is the load ratio (ratio between the maximum load during fatigue test and the average static bond strength of control specimens); N_{cycles} is the number of load cycles; $P_{u,fatigue}$ is the residual static bond strength after 2 million fatigue cycles; $P_{u,fatigue}/P_{u,static}$ is the residual strength ratio.

During fatigue tests of adhesives at high loading frequencies, the temperature of the material usually shows a rising tendency, being this temperature rise higher as the frequency of load increases [25]. For this reason, the temperature in the joint during fatigue testing was registered using two thermocouples (one placed at each face of the specimen), positioned in contact with the CFRP laminate just in the joint centre (Fig. 10). The aim of these measurements was to check that the temperature in the joint due to the high frequency of fatigue loading is well below the glass transition temperature T_g of the adhesive (58ºC), so that this does not affect the strength of the double-strap CFRP-metal joint during testing. In all cases, the maximum temperature increase (compared to room temperature) during testing was below 6.6ºC, which is an acceptable value that do not affect the mechanical properties of the adhesive. Similar results are reported in [26], where the changes in the temperature developed in the adhesive layer of joints under different fatigue loading were insignificant compared to the possible change in the ambient temperature during the test.

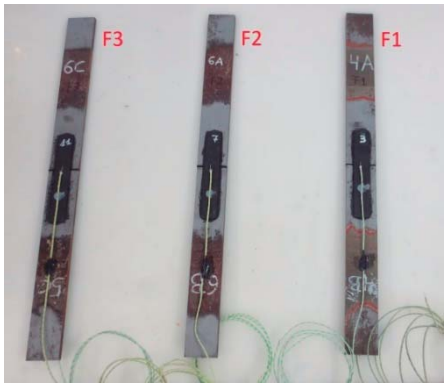

Fig. 10

3.3. Residual stiffness of double strap joints after fatigue loading

To evaluate the stiffness degradation of the adhesive joint subjected to constant cyclic loading, the applied load and crosshead displacement data were recorded during 1 second at a frequency of 175 Hz (175 data points per second) every 100,000 cycles. Based on the data recorded during the fatigue tests, load-extension curves are obtained. Fig. 11 illustrates the fatigue cycles load-extension curves for specimens F1 and F2 at the first cycle, after 1 million cycles and after 2 million cycles, and the curves for F3 at the first cycle, after 200,000 cycles and after 323,000 cycles (at failure).

The stiffness K of the specimen can be defined as the slope of the load-extension curve of the double-strap joint test, $K = \Delta P/\Delta\delta$. The variation in this slope at different load cycles can represent the effect of fatigue loading on the stiffness degradation of the specimen, which is indicative of debonding initiation and propagation [27]. It can be seen from Fig. 11 that the stiffness of all specimens that survived 2 million cycles did not change after fatigue loading (the stiffness of the specimens remained constant for stress ranges of 60 MP in F1 and 75 MPa in F2 in the metallic plates). As a result, it can be concluded that no crack initiation developed in the adhesive joint during fatigue loading at these stress levels, as crack initiation could be considered when K reduces to 90-95% of initial stiffness [27].

As it can be observed from Fig. 11, the hysteretic energy loss during the fatigue cycles of F1 and F2 was minimal. This evidences that the CFRP and the adhesive did not contribute to the heat generation (as measured by thermocouples attached to the CFRP laminates during testing), while the tensile stress in the metallic plates were below the yield point, as also reported in [27] for specimens with modern steel.

However, for the specimen with a stress range of 90 MPa in the metal (F3) and a load ratio $P_{max}/P_{u,static}$ of 0.51, the stiffness reduced 47.41% at the last fatigue cycles before failure (Fig. 11). The observed stiffness reduction is clearly attributed to the immediate development of debonding, as this specimen F3 fails suddenly after 323,384 fatigue cycles.

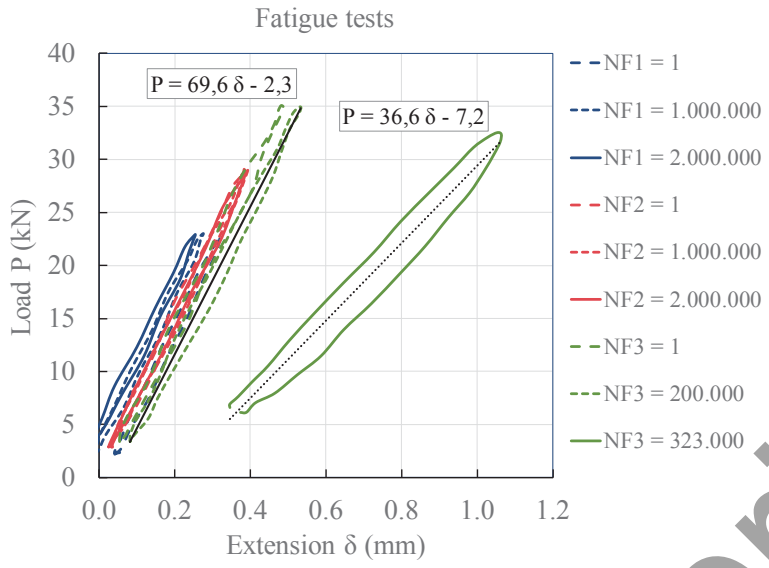

Fig. 11

3.4. Residual bond strength

After fatigue tests, the residual static bond strengths $P_{u,fatigue}$ of specimens which survived 2 million cycles are compared with the static bond strengths of control specimens (Table 4). It is shown that fatigue loading has almost no influence on the residual bond strength, even when the load ratio $P_{max}/P_{u,\ static}$ is 0.42 (F2), as the residual strength ratio $P_{u,fatigue}/\ P_{u,static}$ is close to 1.00 in both cases. Even it is observed a higher residual bond strength for a load ratio of 0.42 (F2) compared to load ratio of 0.33 (F1), but this difference can be attributed to experimental variability. When the load ratio $P_{max}/P_{u,\ static}$ is more than 0.50 (F3), the specimen fails during fatigue test.

3.5. Failure modes

Six different failure modes of CFRP-metal bonded system under tensile loading are proposed by Zhao and Zhang [6]. The comparison of failure modes between static control specimens (S1 and S3), the specimen which survived fatigue loading (F1) and the specimen which failed during fatigue loading (F3) is given in Fig. 12.

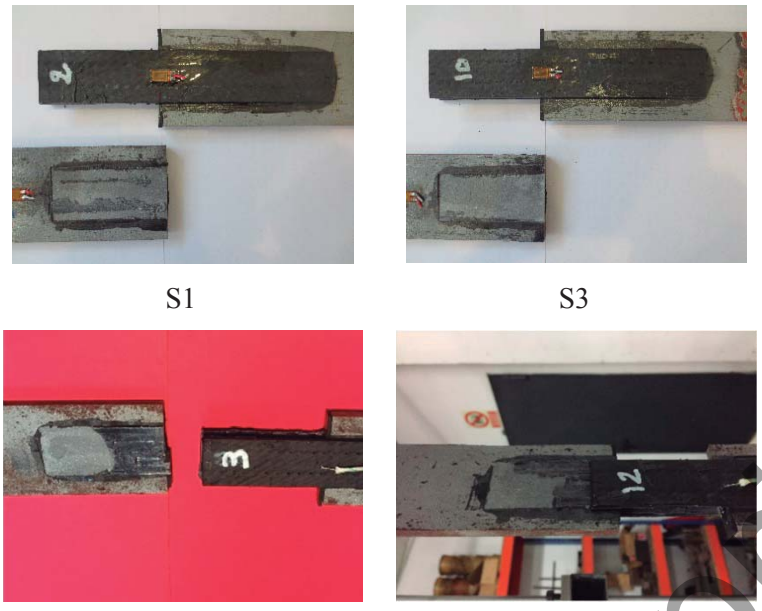

S1 S3

F1 F3

Fig. 12

Concerning the failure mechanism, in control specimens failure mode was mainly metal/adhesive interface debonding, with some adhesive remaining in the metal surface (CFRP/adhesive interface debonding). In the case of fatigue tests, failure mode was mixed with metal/adhesive interface debonding (in the half end of the joint) and CFRP/adhesive interface debonding, with some carbon fibres remaining bonded to the metal. Regarding the expected failure of puddle iron under interlaminar shear, no delamination in the metal surface was observed during these tests. This observation could indicate that the internal laminar structure of this puddle iron is not an issue when considering CFRP strengthening of old bridges. This could be explained by a higher interlaminar shear strength within the metallic plate compared to the shear strength of the adhesive bond between the CFRP laminate and the metallic plate (being the adhesive layer the weakest point). Also, no fatigue damage was observed in the CFRP laminates for these loading levels, as it was expected [14].

3.6. Stress analysis in adhesive

During fatigue tests, CFRP debonding usually starts at stress concentration regions (gap between metallic plates) and propagate along the CFRP/adhesive interfaces [27]. At these fatigue sensitive zones, adhesive shear τ_a and peeling σ_a stresses are higher, so they are regarded as essential parameters to assess the fatigue lifetime of the bond between the metallic plates and the CFRP laminates when failure takes place in the adhesive. Since maximum loads do not exceed the yield stress of the metallic plates, all materials are under linear-elastic behaviour, so an elastic analysis

can be performed to evaluate the stresses in the adhesive layer [6]. The stresses in the adhesive at the gap position are evaluated using the analytical model proposed in [28]:

$$\tau_a = -\frac{1}{b_a}\lambda C_1 \tag{1}$$

$$\sigma_a = \frac{1}{b_a}\left[\frac{a_3 C_1 \lambda^2}{a_1 \lambda^4 + a_2} - 2\beta^2 C_4\right] \tag{2}$$

Where,

$$\lambda = \sqrt{f_2/f_1} \quad , \quad f_1 = \frac{t_a}{G_a b_a} \quad , \quad f_2 = \frac{1}{(EA)_f} + \frac{2}{(EA)_s} \tag{3}$$

$$a_1 = \frac{t_a}{E_a b_a} \quad , \quad a_2 = \frac{1}{(EI)_f} \quad , \quad a_3 = \frac{y_f}{(EI)_f} \quad , \quad \beta^4 = \frac{a_2}{4a_1} \tag{4}$$

$$C_1 = N_{f0} - \frac{P}{f_2 (EA)_s} \quad , \quad C_3 = N_{f0} y_f - \frac{a_3}{a_2 f_2}\frac{P}{(EA)_s} - \frac{a_3 C_1}{a_2 + a_1 \lambda^4} \tag{5}$$

$$C_4 = \frac{1}{\beta}\frac{\lambda a_3 C_1}{a_2 + a_1 \lambda^4} + C_3 \tag{6}$$

where N_{f0} is the tensile force in the CFRP laminates and $y_f = t_f/2$; t_f is the CFRP laminate thickness; b_a is the adhesive width; E_a is the elastic modulus of adhesive; G_a is the shear modulus of adhesive; $(EA)_s$ is the axial stiffness of metallic plate; $(EA)_f$ is the axial stiffness of CFRP laminate; $(EI)_f$ is the bending stiffness of CFRP laminate; and P is the tensile loading during testing. Together with the shear and peeling stresses in the adhesive layer, the maximum principal stress could be evaluated as [27], [29]:

$$\sigma_{ppal} = \frac{\sigma_a}{2} + \sqrt{\left(\frac{\sigma_a}{2}\right)^2 + (\tau_a)^2} \tag{7}$$

Fatigue strength of double-strap joint can be evaluated using the maximum principal stress in the adhesive layer, which develops at the gap between the metallic plates (stress concentration region). This maximum principal stress in the adhesive σ_{ppal} can be used to characterize the failure

in the adhesive layer, as it is assumed to be the governing fatigue stress in the double-strap joint. The maximum principal stress range in the adhesive $\Delta\sigma_{adh}$ is reported in Table 5 for the specimen geometry and material properties considered in the experimental tests, and it is computed as the difference between the maximum principal stresses in the adhesive at P_{max} and P_{min} during the fatigue cycle. As can be seen in Table 4, this stress range in the adhesive layer for specimens that survive 2 million cycles was below the tensile strength of the adhesive (19.0 MPa, see Table 1), but it was not the case when the specimen failed due to fatigue cycles (F3). The higher predicted stress by the analytical model in F3 compared to the tensile strength of the adhesive can be explained by a stress reduction in the real specimens at the gap position, which means that this analytical model produces conservative values of stress levels in the adhesive at the gap location.

Table 5. Fatigue tests parameters.

Spec.	P_{min}	P_{max}	ΔP	$\Delta\sigma_s$	$\Delta\sigma_{adh}$	N_{cycles}
	kN	kN	kN	MPa	MPa	
F-1	2.3	23.0	20.7	60	14.24	2,000,000
F-2	2.9	29.0	26.1	75	16.38	2,000,000
F-3	3.5	35.0	31.5	90	24.72	323,384

4. S-N curve for double-strap joints

In order to obtain an S-N curve representative of CFRP-metal double-strap joints subjected to fatigue loading, a database (126 tests) has been created with results consulted in the literature [27], [30], [31], [32], [33], [34], [35], [36], [37], with similar geometries and test parameters used in tests performed in the present work. The aim is to provide an estimation of the fatigue lifetime of CFRP-metal double-strap joints, and demonstrate that results on puddle iron specimens in the present work are comparable to those with modern steel in literature. This could provide confidence in the use of adhesively-bonded CFRP patches for the strengthening of old metallic bridges.

In Fig. 13, the values of stress range in the metallic plate $\Delta\sigma_s$ (on the y-axis) versus the number of fatigue cycles N (on the x-axis) are represented on logarithmic scale for both axes. These data points correspond to specimens from database and present work that failed during fatigue cycles (32 data points). The double logarithm formula form (power function) shown in eq. (8) is used to describe the S-N curve of adhesively-bonded CFRP-metal double-strap joints.

$$\Delta\sigma_s = 10^{A} N^{-m} \tag{8}$$

where $\Delta\sigma_s$ is the stress range in the metallic plate during fatigue loading, N is the number of fatigue cycles, A and m are constants that can be obtained through a curve fitting to data points by using the least squares method. The mean S-N curve in eq. (9) is computed as the best-fit curve to the data, while the design curve in eq. (10) is considered 1.645 standard deviations below the mean curve, which means that 95% of the results lie above the design curve.

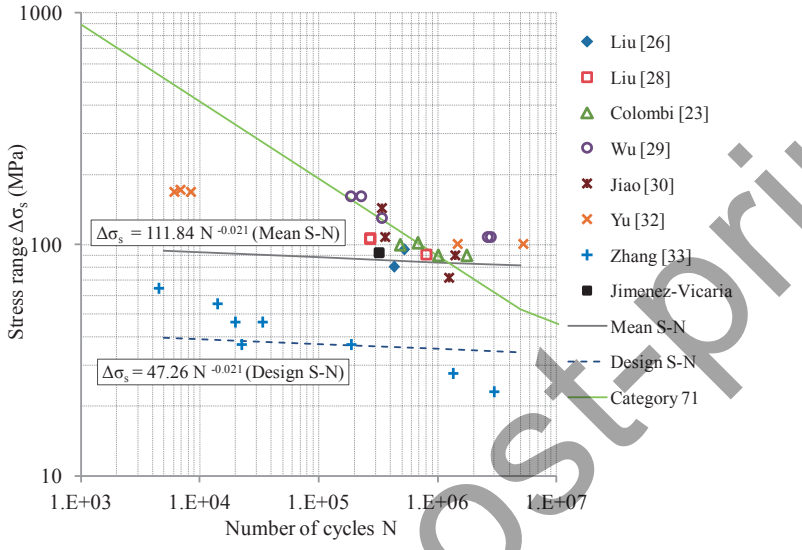

Fig. 13

$$\Delta\sigma_s = 111.84\, N^{-0.021} \text{ (Mean S-N curve)} \quad (9)$$

$$\Delta\sigma_s = 47.26\, N^{-0.021} \text{ (Design S-N curve)} \quad (10)$$

Also, the *category 71* fatigue limit curve for overlapped welded joint detail described in Eurocode 3 (S-N fatigue strength curve for direct stress range of 71 MPa in the steel) is also represented for comparison in Fig. 13, as a good correlation with experimental data on double-strap joints was previously reported in literature [27], [28], [29], [31]. This curve is selected because it represents the fatigue limit of overlapped welded joints with an overlap length 50 mm $\leq l \leq$ 80 mm, similar to the bonded length of CFRP-metal double-strap joints tested. However, it can be seen in Fig. 13 that the fatigue resistance of the CFRP-metal double-strap joints cannot be compared with that of overlapped welded joints (Eurocode 3 design category 71). The slope of the S-N curve for double-straps joints is significantly lower, and also the detail category (defined in Eurocode 3 as the stress range for and endurance of $2\text{x}10^6$ cycles) is 35 MPa in the design S-N curve (well below 71 MPa). This can be explained because the fatigue failure in adhesively-bonded CFRP-metal double-strap joints takes place in the adhesive (or at the interface between adhesive and adherents), but not in the bare metal, so it is more appropriate to consider the S-N curve using the stress range in the

adhesive $\Delta\sigma_{adh}$, instead of the stress range in the metal $\Delta\sigma_s$, for the fatigue evaluation of these double-strap joints.

In a similar way, the S-N curve in Fig. 14 is a plot of $\Delta\sigma_{adh}$ (on the y-axis) versus N (on the x-axis) on logarithmic scales in both axes. For the computation of $\Delta\sigma_{adh}$, the formula in eq. (7) is used. The mean S-N curve in eq. (11) is computed as the best-fit curve to the data, while the design curve in eq. (12) is considered 1.645 standard deviations below the mean curve, which means that 95% of the results lie above the design curve.

$$\Delta\sigma_{adh} = 226.28\ N^{-0.184}\ \textit{(Mean S-N curve)} \tag{11}$$

$$\Delta\sigma_{adh} = 98.71\ N^{-0.184}\ \textit{(Design S-N curve)} \tag{12}$$

From the results of the fatigue life evaluated by stress range in the adhesive $\Delta\sigma_{adh}$, the fatigue limit (for $2\text{x}10^6$ cycles) is considered to be approximately $\Delta\sigma_{adh,limit}$ = 6.8 MPa in the design curve, and 15.7 MPa in the mean curve.

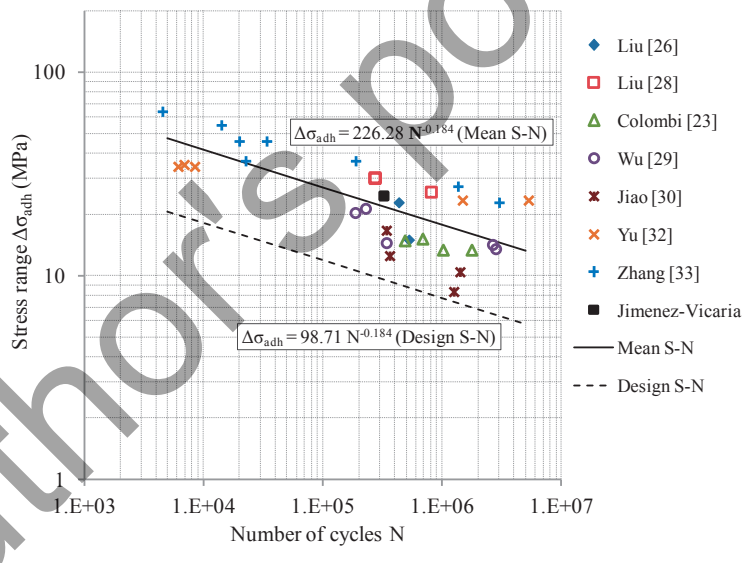

Fig. 14

The fatigue strength curve obtained in Fig. 14 is for a particular category of structural detail (in this case, CFRP-metal double strap joints bonded with epoxy adhesive). Also, it is important to mention that this fatigue strength curve is valid a priori only for specimens with the value ranges of the different properties of the joint specimen in Table 6, until a larger database can be used for a better curve-fitting.

Table 6. Test parameters ranges valid for the proposed fatigue curve.

	$\Delta\sigma_s$	$\Delta\sigma_{adh}$	P_{min}/P_{max}	$P_{max}/P_{u,static}$	E_{CFRP}	t_{CFRP}	l_{CFRP}	E_a	$f_{t,a}$	t_a
	N/mm²	N/mm²			N/mm²	mm	mm	N/mm²	N/mm²	mm
Min	21.60	5.79	0.05	0.18	103500	0.37	60	1451	19.00	0.20
Max	212.40	64.39	0.43	0.80	478730	2.40	250	4500	41.30	1.10

4.1. Residual bond strength after fatigue loading

For the database specimens, the residual strength ratio ($P_{u,fatigue}/P_{u,static}$) is plotted against the load ratio ($P_{max}/P_{u,static}$) in Fig. 15 and the number of fatigue cycles (N_{cycles}) in Fig. 16 to reflect the effect of fatigue loading on the bond strength of double-strap joints. In this case, only the specimens from database that did not fail during fatigue cycles and were subsequently tested under static loading until failure are considered (83 data points). Contrary to the assumption that higher load ratios could reduce the residual strength ratio, it is shown from Fig. 15 that the load ratio has no clear effect on the residual strength ratio. This can be concluded as data points are similarly dispersed (between 0.75 and 1.25) around the unity ($P_{u,fatigue}/P_{u,static} = 1.00$) for the whole range of load ratio values (from 0.18 to 0.62). In a similar way, Fig. 16 shows that the residual strength ratio scatters on both sides of the base line of $P_{u,fatigue}/P_{u,static} = 1.00$, independently on the fatigue cycles the specimens survived before the static testing. Therefore, the observations in Fig. 15 and Fig. 16 indicate that the effect of load ratio and number of cycles on the residual static bond strength of double-strap joints has no clear tendency.

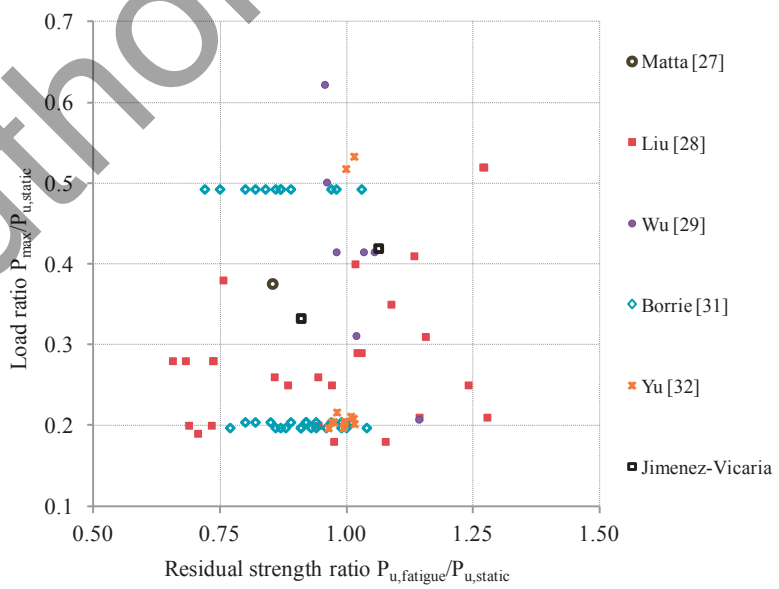

Fig. 15

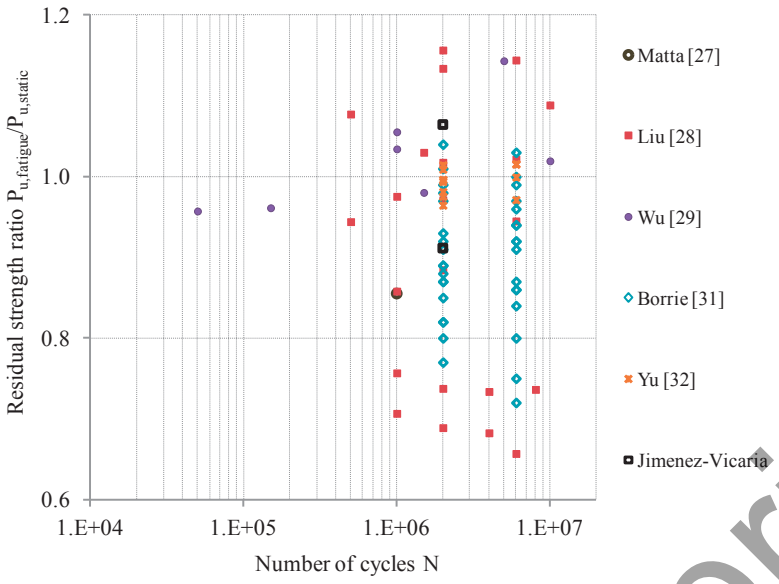

Fig. 16

5. Conclusions

In this paper, the effect of fatigue loading on bond behaviour between CFRP laminates and puddle iron plates taken from an old railway bridge is investigated. The following conclusions can be drawn, based on the experimental observations:

- The particular properties of puddle iron seems to not affect the static bond strength of double-strap joints, as specimens with puddle iron had an average static bond strength consistent with results on modern steel specimens with the same geometry and same CFRP and adhesive. Also, these particular properties of puddle iron did not influence the effect of fatigue loading on the bond behaviour between CFRP and the puddle iron specimens, even when the load ratio was 0.42 (F2), as the residual strength ratio is close to 1.00. However, the number of tests with puddle iron is limited, so more tests should be performed in the future to confirm this.
- The temperature in the joint due to the high frequency of fatigue loading (10 Hz) was well below the glass transition temperature T_g of the adhesive, so this did not affect the strength of the double-strap CFRP-metal joint during fatigue testing (maximum temperature increase of 6.6ºC is measured, comparable to the possible change in room temperature).
- The stiffness of puddle iron specimens that survived 2 million cycles (F1 and F2) did not change after fatigue loading, so no crack initiation was expected in the adhesive at load ratios below 0.42 (F2). For specimen tested under a load ratio of 0.51 (F3), a clear stiffness reduction (47.41%) was observed just before fatigue failure, attributed to the sudden development of debonding.

- The failure mode of puddle iron double-strap joints subjected to fatigue loading was similar to the observed in modern steel ones: metal/adhesive interface debonding and CFRP/adhesive interface debonding. No delamination under interlaminar shear within the puddle iron plates was observed after fatigue, so it can be said that CFRP strengthening could be applied to this puddle iron, although a more extense experimental campaign should be done to confirm this.
- Based on experimental results, an S-N fatigue curve is obtained for CFRP-metal double-strap specimens, and a fatigue limit in terms of maximum principal stress range in the adhesive layer $\Delta\sigma_{adh}$ is proposed to be used in design guidelines. The fatigue limit, defined for $2x10^6$ cycles in the design curve, is considered to be approximately $\Delta\sigma_{adh,limit} = 6.8$ MPa.

Further work should be performed in order to provide a larger database of fatigue data with puddle iron specimens, so a more accurate estimation of the fatigue lifetime of CFRP-metal double-strap joints with puddle iron can be obtained.

Acknowledgements

The research leading to these results has received partial funding from the European Union's Horizon 2020 Programme in the framework of the research project IN2TRACK under grant agreement n° 730841. The authors also wish to thank the laboratory technicians of ACCIONA Construction Technological Centre, where static tests were carried out, and the Laboratory of Science and Engineering of Materials of the University of Cantabria (LADICIM) where fatigue tests were carried out. Also, we want to mention that the mechanical and chemical characterization of puddle iron was performed by UTE SERS-TAM, and data was provided by the Technical Division of the General Directorate of Conservation and Maintenance of Adif (Spanish Railway Administrator).

Data Availability

The raw/processed data required to reproduce these findings cannot be shared at this time due to technical or time limitations.

527 **References**

528

529 [1] Ghafoori, E., Hosseini, A., Al-Mahaidi, R., Zhao, X.L., Motavalli, M. Prestressed CFRP-
530 strengthening and long-term wireless monitoring of an old roadway metallic bridge. Engineering
531 Structures, 176 (2018), 585–605.
532 [2] Robert J. Dexter and Justin M. Ocel. Manual for repair and retrofit of fatigue cracks in steel
533 bridges. FHWA Publication No. FHWA-IF-13-020. March 2013.
534 [3] Pipinato, A., Pellegrino, C. and Modena, C. Fatigue Behaviour of Steel Bridge Joints
535 Strenghtened with FRP Laminates. Modern Applied Science; Vol. 6, No. 10; 2012.
536 [4] Hollaway LC, Cadei J. Progress in the technique of upgrading metallic structures with
537 advanced polymer composites. Prog Struct Mat Eng 2002;4(2):131–48.
538 [5] Cadei JMC, Stratford TJ, Hollaway LC, Duckett WH. C595 -Strengthening metallic structures
539 using externally bonded fibre-reinforced composites. London: CIRIA; 2004.
540 [6] Zhao XL, Zhang L. State of the art review on FRP strengthened steel structures. Eng Struct
541 2007;29(8):1808–23.
542 [7] Schnerch D, Dawood M, Rizkalla S, Sumner E. Proposed design guidelines for strengthening
543 of steel bridges with FRP materials. Construction and Building Materials, 2007;21(5):1001–10.
544 [8] A. Shaat, D. Schnerch, A. Fam, S. Rizkalla, "Retrofit of Steel Structures Using Fiber
545 Reinforced Polymers (FRP): State-of-the-Art", Transportation Research Board (TRB) Annual
546 Meeting, DC, USA Washington, 2004.
547 [9] J.M.C. Cadei, T.J. Stratford, W.G. Duckett, L.C. Hollaway, Strengthening metallic structures
548 using externally bonded fibre-reinforced polymers, Constr. Ind. Res. Inf. Assoc. (2004).
549 [10] Jones SC, Civjan SA. Application of fibre reinforced polymer overlays to extend steel fatigue
550 life. J Compos Construct 2003;7(4):331–8.
551 [11] Deng J, Lee MMK. Fatigue performance of metallic beam strengthened with a bonded CFRP
552 plate. Compos Struct 2007;78:222–31.
553 [12] Taljsten B, Hansen CS, Schmidt JW. Strengthening old metallic structures in fatigue with
554 prestressed and non-prestressed laminates. Constr Build Mater 2009;23:1665–77.
555 [13] E. Lepretre, S. Chataigner, L. Dieng, L. Gaillet. Fatigue strengthening of cracked steel plates
556 with CFRP laminates in the case of old steel material. Construction and Building Materials 174
557 (2018) 421–432.
558 [14] Thomas Jollivet, Catherine Peyrac, Fabien Lefebvre. Damage of composite materials.
559 Procedia Engineering, 66 (2013), 746- 758.
560 [15] Moy, S.s.J.. (2014). Strengthening of historic metallic structures using fibre-reinforced
561 polymer (FRP) composites. In book: Rehabilitation of Metallic Civil Infrastructure Using Fiber
562 Reinforced Polymer (FRP) Composites, pp.406-429.

563 [16] Eurocode 3 – Design of Steel Structures – Part 1–9: Fatigue. European Committee for
564 Standardization (CEN); 2005.
565 [17] Jimenez-Vicaria, J. David, G. Pulido, M. Dolores and Castro-Fresno, Daniel. Influence of
566 carbon fibre stiffness and adhesive ductility on CFRP-steel adhesive joints with short bond
567 lengths. Construction and Building Materials (pending for publication).
568 [18] Fernando, D., Teng, J. G., Yu, T. and Zhao, X. L. 2013. Preparation and Characterization of
569 Steel Surfaces for Adhesive Bonding. Journal of Composites for Construction, 17(6), 04013012.
570 [19] UNE-EN 6892-1. Metallic materials - Tensile testing - Part 1: Method of test at room
571 temperature.
572 [20] UNE-EN ISO 148. Metallic materials - Charpy pendulum impact test.
573 [21] Lacalle, R., Álvarez, J.A., Ferreño, D. et al. Influence of the Flame Straightening Process on
574 Microstructural, Mechanical and Fracture Properties of S235 JR, S460 ML and S690 QL
575 Structural Steels. Exp Mech 53, 893–909 (2013).
576 [22] ASTM D3039/D3039M-08. Tensile properties of polymer matrix composite materials.
577 American Society for Testing and Materials; 2008.
578 [23] ASTM D638 - 14. Standard test method for tensile properties of plastics. American Society
579 for Testing and Materials; 2008.
580 [24] UNE-EN 10025-2. Hot rolled products of structural steels - Part 2: Technical delivery
581 conditions for non-alloy structural steels.
582 [25] Andrzej Komorek, Zenon Komorek, Aneta Krzyzak, Pawel Przybylek, Robert Szczepaniak.
583 Impact of Frequency of Load Changes in Fatigue Tests on the Temperature of the Modified
584 Polymer. Int J Thermophys (2017) 38:128.
585 [26] Olajide, Sheriff.O., Arhatari, B.D., Progress on interacting fatigue, creep & hysteretic heating
586 in polymer adhesively bonded composite joints, International Journal of Fatigue (2017).
587 [27] Pierluigi Colombi, Giulia Fava. Fatigue behaviour of tensile steel/CFRP joints. Composite
588 Structures 94 (2012) 2407–2417.
589 [28] Bocciarelli M, Colombi P, Fava G, Poggi C. Fatigue performance of tensile steel members
590 strengthened with CFRP plates. Compos Struct 2009;87:334–43.
591 [29] Thay, V., Nakamura H. and S. Tezuka. Evaluation of fatigue durability of adhesively bonded
592 joints between steel plate and CFRP laminates. Proceedings of the Eighth International
593 Conference on Fibre-Reinforced Polymer (FRP) Composites in Civil Engineering, CICE 2016,
594 Hong Kong, China.
595 [30] H.B. Liu, X.L. Zhao and R. Al-Mahaidi. The effect of fatigue loading on bond strength of
596 CFRP bonded steel plate joints. In: Proceedings of the International Symposium on Bond
597 Behaviour of FRP in Structures (BBFS 2005).

[31] Matta, F.; Karbhari, Vistasp M.; and Vitaliani, Renato. Tensile Response of Steel/CFRP Adhesive Bonds for the Rehabilitation of Civil Structures. Structural and Engineering Mechanics, Vol. 20, No. 5 (2005) 589-608.

[32] H. B. Liu, X. L. Zhao and Al-Mahaidi. Effect of fatigue loading on bond strength between CFRP sheets and steel plates. International Journal of Structural Stability and Dynamics, Vol. 10, No. 1 (2010) 1-20.

[33] Wu C, Zhao XL, Chiu WK, Al-Mahaidi R, Duan WH. Effect of fatigue loading on the bond behaviour between UHM CFRP plates and steel plates. Compos Part B: Eng 2013;50:344–53.

[34] H. Jiao, H., Phan, H.B. and Zhao, X.L. Fatigue Behaviour of Steel Elements Strengthened with Stand CFRP Sheets. Advances in Structural Engineering Vol. 17 No. 12, 2014.

[35] D. Borrie, H.B. Liu, X.L. Zhao, R.K. Singh Raman, Y. Bai. Bond durability of fatigued CFRP-steel double-lap joints pre-exposed to marine environment. Composite Structures 131 (2015) 799–809.

[36] Qian-Qian Yu, Rui-Xin Gao, Xiang-Lin Gu, Xiao-Ling Zhao, Tao Chen. Bond behavior of CFRP-steel double-lap joints exposed to marine atmosphere and fatigue loading. Engineering Structures 175 (2018) 76–85.

[37] Zhang, L., Cao, S. and Tao, X. Experimental Study on Interfacial Bond Behavior between CFRP Sheets and Steel Plates under Fatigue Loading. Materials 2019, 12, 377.

Figures captions

Fig. 1. Schematic view of the double-strap joint specimen (not to scale).

Fig. 2. Puddle iron plates cut from the web of riveted stringers of Redondela bridge.

Fig. 3. Specimens preparation.

Fig. 4. Micrographs of puddle iron plates from Redondela Bridge (various magnifications).

Fig. 5. Stress-strain curves of materials.

Fig. 6. Test setup and instrumentation for specimens under static loading.

Fig. 7. Load–CFRP strain curve for static specimens.

Fig. 8. Test setup and instrumentation for specimens under fatigue loading.

Fig. 9. Load–extension curves for static tests after fatigue loading in specimens F1 and F2 (which survived 2 million cycles).

Fig. 10. Fatigue specimens monitored with thermocouples.

Fig. 11. Load–extension cyclic curves for fatigue specimens F1, F2 and F3 at different cycles.

Fig. 12. Failure modes of double-strap joints.

Fig. 13. S-N curve in logarithmic representation for double-strap joints in database and present work (stress range in the metal $\Delta\sigma_s$).

Fig. 14. S-N curve in logarithmic representation for double-strap joints in database and present work (maximum principal stress range in the adhesive $\Delta\sigma_{adh}$).

Fig. 15. Effect of load ratio on the residual strength ratio of double-strap joints.

Fig. 16. Effect of fatigue loading on the residual static bond strength of double-strap joints.